

See discussions, stats, and author profiles for this publication at: <https://www.researchgate.net/publication/8385517>

# Car Exhaust Catalysis from First Principles: Selective NO Reduction under Excess O<sub>2</sub> Conditions on Ir

ARTICLE *in* JOURNAL OF THE AMERICAN CHEMICAL SOCIETY · OCTOBER 2004

Impact Factor: 12.11 · DOI: 10.1021/ja0481833 · Source: PubMed

---

CITATIONS

84

---

READS

21

3 AUTHORS, INCLUDING:



Zhi-Pan Liu

Fudan University

110 PUBLICATIONS 4,460 CITATIONS

SEE PROFILE



Stephen John Jenkins

University of Cambridge

151 PUBLICATIONS 2,850 CITATIONS

SEE PROFILE

## Car Exhaust Catalysis from First Principles: Selective NO Reduction under Excess O<sub>2</sub> Conditions on Ir

Zhi-Pan Liu, Stephen J. Jenkins, and David A. King\*

*Contribution from the Department of Chemistry, University of Cambridge, Lensfield Road, Cambridge CB2 1EW, U.K.*

Received March 30, 2004; E-mail: dak10@cam.ac.uk

**Abstract:** Combining energetic data from density functional theory with thermodynamic calculations, we have studied in detail selective NO reduction under excess O<sub>2</sub> conditions on Ir. We show that excess O<sub>2</sub> can readily poison the Ir catalyst for NO reduction and the poisoning starts from a low O coverage on the surface. The adsorbed O switches the reaction selectivity from reduction (N<sub>2</sub> production) to oxidation (NO<sub>2</sub> production). As the O coverage is built up, Ir metal can eventually be oxidized to IrO<sub>2</sub>, which is predicted to be thermodynamically possible under reaction conditions. To prevent O poisoning the surface, the presence of reductants is thus essential. We demonstrate that NO reduction is sensitive to the choice of reductant, and that alkenes are the most effective, mainly because they are able to produce surface C atoms that can selectively remove O atoms from Ir steps. On the basis of our analyses of the electronic structures, the mechanism of O-poisoning is elucidated and the reactant sensitivity in NO reduction is also discussed in terms of the bonding competition effect. We found that for different adsorbates, such as NO, O, and N, their bondings with surface d-states are remarkably similar. This gives rise to an indirect repulsion between adsorbates whenever they may bond with the same metal atoms. This energy cost can be qualitatively correlated with the valency of the adsorbate, and this is the key to understand the O-poisoning effect and the structure sensitivity in NO reduction.

### 1. Introduction

Nitric oxide is a molecule of considerable scientific interest, not least because of its rich chemical properties.<sup>1–3</sup> Technologically, NO is involved in many industrial processes, such as ammonia oxidation (NO is oxidized into HNO<sub>3</sub>) and emissions control (NO is reduced into N<sub>2</sub>). In the past two decades, NO removal has received much attention due to growing concerns over the pollution caused by vehicle exhausts. To date, no best solution has been found for NO removal under excess O<sub>2</sub> conditions, which is encountered in the after-treatment of exhaust gases from energy-efficient engines, such as diesel and lean-burn gasoline engines.<sup>4,5</sup> It is the oxidizing environment that increases considerably the difficulty of NO reduction. Despite extensive experimental studies devoted to this problem,<sup>4–17</sup> many fundamental issues are still much in debate.<sup>4,5</sup>

For instance, what is the physical origin of the catalyst poisoning due to the excess O<sub>2</sub>? How can NO be reduced rather than oxidized in an oxidizing environment? In this paper we aim to address these puzzles using first-principles density functional theory (DFT) and thermodynamic calculations.

An important finding in experimental studies of selective NO reduction under excess O<sub>2</sub> conditions is that when *hydrocarbons* are present, platinum group metals (e.g. Pt, Ir, Rh, Pd, Co) become active in reducing NO to N<sub>2</sub>.<sup>6–8</sup> An appealing feature in this approach is that hydrocarbons are required only in small quantities, in contrast to the large excess of O<sub>2</sub>. Experimental studies have shown that the activity and the selectivity of the process depend very much on the metal species. To obtain a catalyst with both high activity and high selectivity has proved to be extremely difficult. For example, Pt catalysts were found to be very active for NO reduction at low temperatures, but their selectivity to N<sub>2</sub> production is rather poor (aside from N<sub>2</sub>, N<sub>2</sub>O is another major product).<sup>4,5,9</sup>

In the past few years, it has been reported that Ir can be highly active *and* selective to reduce NO to N<sub>2</sub> when it is present in the form of nanoparticles (e.g. 40–60 nm).<sup>10–15</sup> This is quite unexpected, considering that Ir bulk metals were long known to be of low activity. In addition to the structure sensitivity,<sup>13,14</sup> the performance of NO reduction on Ir is also sensitive to the presence of reductants.<sup>4,15</sup> Without reductants, or with reductants

- (1) Chalasinski, G.; Szczesniak, M. N. *Chem. Rev.* **1994**, *94*, 1723.
- (2) Stirling, A.; Papai, I.; Mink, J.; Salahub, D. R. *J. Chem. Phys.* **1994**, *100*, 2910.
- (3) Brown, A. W.; King, D. A. *J. Phys. Chem.* **2000**, *104*, 2578.
- (4) Parvulescu, V. I.; Grange, P.; Delmon, B. *Catal. Today* **1998**, *46*, 233.
- (5) Burch, R.; Breen, J. P.; Meunier, F. C. *Appl. Catal. B* **2002**, *39*, 283.
- (6) Hamada, H.; Kintaichi, Y.; Sasaki, M.; Ito, T. *Appl. Catal.* **1991**, *75*, L1.
- (7) Obuchi, A.; Ohi, A.; Nakamura, M.; Ogata, K.; Mizuno, N.; Ohuchi, H. *Appl. Catal. B* **1993**, *2*, 71.
- (8) Iwamoto, M.; Yahiro, H.; Shundo, S.; Yu-u, Y.; Mizuno, N. *Shokubai (Catalyst)* **1990**, *32*, 430.
- (9) Burch, R.; Millington, P. *Catal. Today* **1996**, *29*, 37.
- (10) Taylor, K. C.; Schlatter, J. C. *J. Catal.* **1980**, *63*, 53.
- (11) Tauster, S. L.; Murell, L. L. *J. Catal.* **1976**, *41*, 192.
- (12) Nawdali, M.; Iojoiu, E.; Gelin, P.; Praliaud, H.; Primet, M. *Appl. Catal. A* **2001**, *220*, 129.
- (13) Nakatsuji, T. *Appl. Catal. B* **2000**, *25*, 163.
- (14) Wogerbauer, C.; Maciejewski, M.; Baiker, A. *J. Catal.* **2002**, *205*, 157.

- (15) Wogerbauer, C.; Maciejewski, M.; Baiker, A. *Appl. Catal. B* **2001**, *34*, 11.
- (16) Burch, R.; Watling, T. C. *Catal. Lett.* **1996**, *37*, 51.
- (17) Konsolakis, M.; Macleod, N.; Isaac, J.; Yentekakis, I. V.; Lambert, R. M. *J. Catal.* **2000**, *193*, 330.

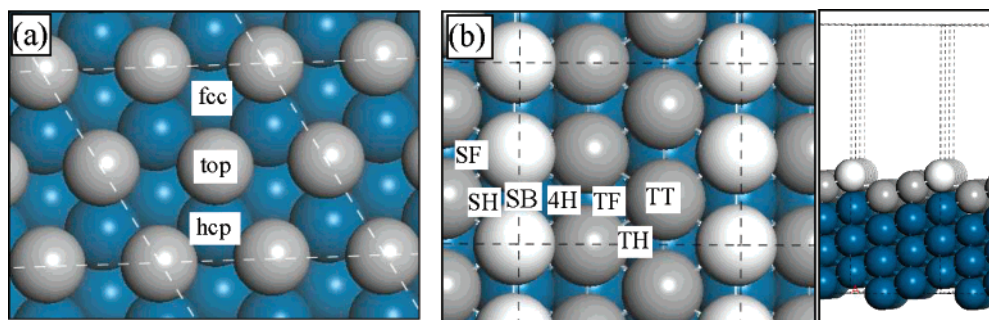


**Figure 1.** Slab structures of the flat Ir{111} (a) and the stepped Ir{211} (b) used in the DFT modeling. The high-symmetry sites on the surfaces have been labeled. The side view of the {211} surface is also shown. The labels SF, SH, SB, 4H, TF, TH, and TT in (b) stand for step-fcc, step-hcp, step-bridge, four-fold-hollow, terrace-fcc, terrace-hcp, and terrace-top, respectively.

such as CO, H<sub>2</sub>, and alkanes, NO cannot be well reduced but is mainly oxidized to NO<sub>2</sub>. In contrast, alkenes such as propene can work well in assisting NO-to-N<sub>2</sub> conversion. Since the oxide form of Ir (IrO<sub>2</sub>) was found to be unreactive for NO reduction, it has been suspected that the reductant sensitivity is due to the different ability of reductants to reduce the oxidized form of Ir. However, recent experiment<sup>13</sup> countered this argument by showing that the reductants CO, H<sub>2</sub>, and hydrocarbons work equally well in reducing IrO<sub>2</sub> into Ir metal. An alternative explanation lies in the fact that alkenes are able to produce more carbonaceous (C<sub>x</sub>H<sub>y</sub>) species on the surface, which may assist the decomposition of NO.<sup>4,13,16</sup>

It is now generally accepted that the NO reduction process on platinum group metals consists of the following steps:<sup>4,5</sup> (i) NO dissociation (NO → N + O); (ii) N<sub>2</sub> formation (N + N → N<sub>2</sub>); (iii) byproducts, N<sub>2</sub>O, and NO<sub>2</sub> formations (NO + N → N<sub>2</sub>O, NO + O → NO<sub>2</sub>); and (iv) O-removal reactions. Only in recent years have DFT calculations been utilized to understand the mechanisms of the individual elementary steps.<sup>18,20–22</sup> Most of the calculations<sup>18</sup> were, however, focused on the first step, the NO dissociation. It was found that NO dissociation on transition metals occurs preferentially in monatomic steps, consistent with experimental observations.<sup>19</sup> Similar structure sensitivity for the N + N → N<sub>2</sub> reaction on Pd surfaces has been reported by Hammer.<sup>20</sup> Burch et al.<sup>21</sup> have calculated the NO + N → N<sub>2</sub>O and NO + O → NO<sub>2</sub> reactions on Pt{111}. Very recently, we studied systematically NO dissociation and the N<sub>2</sub>, N<sub>2</sub>O, and NO<sub>2</sub> formation reactions on Ir and Pt surfaces, including flat {111} and stepped {211} surfaces.<sup>22</sup> We found that only the stepped Ir{211} surface possesses both high activity and high selectivity for the NO reduction; the other surfaces, including both Pt surfaces and the flat Ir{111} surface, lack either the activity or the selectivity, or both. These results explained the observed metal dependency and the structure sensitivity of the NO reduction.

To date, the complete mechanism of selective NO reduction has not been established. Fundamentally, it remains unclear how the excess O<sub>2</sub> poisons the NO reduction in the absence of reductants, or in the presence of only the ineffective reductants, such as CO and H<sub>2</sub>. And it is also natural to ask why certain reductants, such as alkenes, can prevent the O<sub>2</sub> poisoning,

considering that they are in much lower concentration than O<sub>2</sub>. These questions are of fundamental importance because the poisoning and the activation of metal catalysts are central issues in heterogeneous catalysis. In this work we investigate how NO reduction on Ir surfaces is achieved under excess O<sub>2</sub> conditions, focusing on the interplay of excess O<sub>2</sub>, reductants, and Ir metal surfaces. First-principles DFT calculations in combination with thermodynamic calculations were applied to address the following two key issues: (i) the poisoning effects of excess O<sub>2</sub> and (ii) the microscopic mechanism of the O-removal reactions by reductants.

Our calculations show that the excess O<sub>2</sub> has a severe poisoning effect on NO reduction. Even a low coverage of O atoms on the surface can poison the reaction by switching the selectivity. The presence of surface C atoms that may derive from hydrocarbons plays the key role in activating the poisoned Ir surface, which explains the observed reductant sensitivity of NO reduction.

## 2. Calculation Methods

Two Ir surfaces with different structures (flat Ir{111} and stepped Ir{211}, shown in Figure 1) have been chosen to model selective NO reduction on Ir under excess O<sub>2</sub> conditions. The close-packed {111} facet is generally the dominant face in real face-centered-cubic (fcc) metal catalyst particles, and the monatomic steps possessed by the {211} facet are possibly the most common defects.<sup>19,23</sup> For this reason, these two surfaces have been most often used to model real catalytic processes.<sup>18,20,24,25</sup> Our previous work<sup>22</sup> also showed that these two surfaces are able to describe the essential catalytic features, e.g. the activity and the selectivity of NO reduction on Ir and Pt.

Total energy calculations were performed using the DFT-slab approach<sup>26</sup> with the GGA-PW91<sup>27</sup> functional. The Ir{111} surfaces were modeled by a 4-layer slab with the top layer relaxed; the Ir{211} surfaces were modeled by 12-layer slabs with the top three layers relaxed (see Figure 1). The electronic wave functions were expanded in a plane wave basis set, and the ionic cores were described by ultrasoft pseudopotentials.<sup>28</sup> The vacuum region between slabs was 10 Å, and a cutoff energy of 340 eV was used. Monkhorst–Pack *k*-point sampling with approximately 0.07 Å<sup>−1</sup> spacing was utilized for all of the calculations (for example, for a *p*(2×2) Ir{111} slab, 3 × 3 × 1 *k*-point

- (18) Hammer, B. *Phys. Rev. Lett.* **1999**, 83, 3681. Loffreda, D.; Simon, D.; Sautet, P. *J. Catal.* **2003**, 213, 211. Eichler, A.; Hafner, J. *J. Catal.* **2001**, 204, 118.  
 (19) Zambelli, T.; Wintterlin, J.; Trost, J.; Ertl, G. *Science* **1996**, 273, 1688.  
 (20) Hammer, B. *J. Catal.* **2001**, 199, 171.  
 (21) Burch R.; Daniells, S. T.; Hu, P. *J. Chem. Phys.* **2002**, 117, 2902.  
 (22) Liu, Z.-P.; Jenkins, S. J.; King, D. A. *J. Am. Chem. Soc.* **2003**, 125, 14660

- (23) (a) Somorjai, G. A. *Introduction To Surface Chemistry And Catalysis*; John Wiley & Sons Inc.: New York, 1994. (b) Somorjai, G. A. *J. Mol. Struct. (THEOCHEM)* **1998**, 424, 101.  
 (24) Liu, Z.-P.; Hu, P.; Alavi, A. *J. Am. Chem. Soc.* **2002**, 124, 14770.  
 (25) Liu, Z.-P.; Hu, P. *J. Am. Chem. Soc.* **2003**, 125, 1958.  
 (26) CASTEP 4.2, academic version, licensed under UKCP–Accelrys. Payne, M. C.; Teter, M. P.; Allan, D. C.; Arias, T. A.; Joannopoulos, J. D. *Rev. Mod. Phys.* **1992**, 64, 1045.  
 (27) Perdew, J. P.; Chevary, J. A.; Vosko, S. H.; Jackson, K. A.; Pederson, M. R.; Singh, D. J.; Fiolhais, C. *Phys. Rev. B* **1992**, 46, 6671.  
 (28) Vanderbilt, D. *Phys. Rev. B* **1990**, 41, 7892.

sampling is used). The accuracy of the DFT-slab approach has previously been benchmarked against individual experiments on the adsorption structures and bond energies of numerous other systems,<sup>29</sup> giving us confidence in our results.

The transition states (TSs) of all the reactions studied were searched for using a constrained minimization technique, in which all the degrees of freedom of the system except the reaction coordinate (the bond being formed/broken) are relaxed. The TS was identified when (i) the forces on the atoms vanish and (ii) the energy is a maximum along the reaction coordinate, but a minimum with respect to all of the remaining degrees of freedom. It should be mentioned that, in the study of the O-poisoning effect on the surface reactions, we have explored the most likely TS configurations by varying the positions of the coadsorbed O and the TS complex, and the most stable TS thus identified was then used to calculate the reaction barrier. Previous work<sup>24,25</sup> has demonstrated that the above DFT setup affords a good accuracy, especially for the calculation of reaction barriers in heterogeneous catalysis (usually within 0.1 eV).

### 3. Results

**3.1. Thermodynamic Aspects of the O Coverage and the Possibility of Oxide Formation.** There are two important issues that may first be considered for a metal catalyst in excess O<sub>2</sub> conditions: the O coverage on metal surfaces and the possibility of oxide formation. Both of them modify the nature of the surface and thus may not be conducive to the desired reactions. To examine these two issues, we applied thermodynamic equations to a simplified system consisting only of O<sub>2</sub> and Ir metal. Since the other exhaust components, such as NO, CO, and hydrocarbons, are much lower in concentration than O<sub>2</sub>, they are not taken explicitly into account. The temperature (*T*) and the O<sub>2</sub> pressure (*p*) of the system are set to be 600 K and 0.08 atm, respectively, according to the typical experimental conditions for Ir catalysts.

**(a) O<sub>2</sub> Adsorption:**  $\frac{1}{2}\text{O}_2(\text{g}) + \text{Sur}(\text{s}) \rightarrow \text{O}/\text{Sur}(\text{s})$ . At the given *T* and *p*, the change in Gibbs free energy per additional O adatom due to the O<sub>2</sub> adsorption process may be written as where  $G_n^{\text{sur}}(T, p)$  is the free energy of the surface plus *n*

$$\delta G_{\text{ads}}(T, p) = G_{n+1}^{\text{sur}}(T, p) - G_n^{\text{sur}}(T, p) - \mu_{\text{O}}(T, p) \quad (1)$$

adsorbed O atoms. The chemical potential  $\mu_{\text{O}}(T, p)$  is that of the O atom in the gas phase, which is defined to be half of the gas-phase O<sub>2</sub> chemical potential,  $\mu_{\text{O}_2}(T, p)$ . For the solid states, the DFT-calculated total energy,  $E_n^{\text{sur}}$  (strictly speaking, the Helmholtz free energy at 0 K and neglecting zero-point vibrations), is used to represent the corresponding Gibbs free energy at finite *T* and *p*,  $G_n^{\text{sur}}(T, p)$ . This approximation is justified because the corresponding corrections that enter into  $\delta G_{\text{ads}}(T, p)$  are small (see refs 31 and 32). The chemical potential  $\mu_{\text{O}}(T, p)$  can be correlated with the standard state ( $T, p^\circ = 10^5 \text{ Pa} = 1 \text{ bar}$ ) as follows:

$$\mu_{\text{O}}(T, p) = \frac{1}{2}\mu_{\text{O}_2}(T, p) = \frac{1}{2}\{\mu_{\text{O}_2}(T, p^\circ) + RT \ln(p/p^\circ)\} \quad (2)$$

To calculate the  $\mu_{\text{O}_2}(T, p^\circ)$ , a zero reference state of  $\mu_{\text{O}_2}$  needs to be defined; here we set the total energy of an O<sub>2</sub> molecule in

the gas phase (including zero-point energy) to be zero:  $E_{\text{O}_2} \equiv 0$ . From this reference point, we get  $H_{\text{O}_2}(T^\circ, p^\circ) = \Delta H_{\text{O}_2}(0 \rightarrow T^\circ, p^\circ)$ , as  $H_{\text{O}_2}(0 \text{ K}, p^\circ) \approx 0$ . The data of  $\Delta H_{\text{O}_2}(0 \rightarrow T^\circ, p^\circ)$  are tabulated in the literature.<sup>33</sup> Now we can expand  $\mu_{\text{O}_2}(T, p^\circ)$  as

$$\begin{aligned} \mu_{\text{O}_2}(T, p^\circ) &= H_{\text{O}_2}(T, p^\circ) - \text{TS}_{\text{O}_2}(T, p^\circ) \\ &= (H_{\text{O}_2}(T, p^\circ) - H_{\text{O}_2}(T^\circ, p^\circ)) - \text{TS}_{\text{O}_2}(T, p^\circ) + H_{\text{O}_2}(T^\circ, p^\circ) \\ &= \Delta H_{\text{O}_2}(T^\circ \rightarrow T, p^\circ) - \text{TS}_{\text{O}_2}(T, p^\circ) + \Delta H_{\text{O}_2}(0 \rightarrow T^\circ, p^\circ) \quad (3) \end{aligned}$$

By using the experimental data ( $\Delta H_{\text{O}_2}$  and  $S_{\text{O}_2}$ ) in the literature,<sup>33</sup>  $\mu_{\text{O}_2}(T, p^\circ)$  can be computed. Combining (2) and (3), we obtain  $\mu_{\text{O}}(600 \text{ K}, 0.08 \text{ atm}) = -0.68 \text{ eV}$ . As  $\mu_{\text{O}}$  is now known, we return to eq 1:

$$\begin{aligned} \delta G_{\text{ads}}(T, p) &= E_{n+1}^{\text{sur}} - E_n^{\text{sur}} - \mu_{\text{O}}(T, p) = (E_{n+1}^{\text{sur}} - E_n^{\text{sur}} - E_{\text{O}}) + (E_{\text{O}} - 0.5E_{\text{O}_2}) - \mu_{\text{O}}(T, p) \\ &= -E_{\text{ad}}^{\text{diff}} + \frac{1}{2}E_{\text{bond}}(\text{O}_2) - \mu_{\text{O}}(T, p) \quad (4) \end{aligned}$$

where  $E_{\text{bond}}(\text{O}_2)$  is the gas-phase O<sub>2</sub> bonding energy, which is 5.58 eV from our DFT calculation (zero-point energy is included).  $E_{\text{ad}}^{\text{diff}} = -(E_{n+1}^{\text{sur}} - E_n^{\text{sur}} - E_{\text{O}}) = -(dE/dn)|_\theta$  is the differential adsorption energy with respect to an isolated gas-phase O atom (i.e., the coverage-dependent change in total energy upon adsorption of a single additional O atom). If the O<sub>2</sub> adsorption equilibrium can be reached, we must have  $\delta G_{\text{ads}}(T, p) = 0$ , so from eq 4 we can obtain that  $E_{\text{ad}}^{\text{diff}} = 3.47 \text{ eV}$  at 600 K and 0.08 atm.

**(b) Oxide Formation Process:**  $\text{O}_2(\text{g}) + \text{Ir}(\text{s}) \rightarrow \text{IrO}_2(\text{s})$ . At the given *T* and *p*,  $\delta G_{\text{ox}}(T, p)$  of the Ir oxide formation process can be written as

$$\delta G_{\text{ox}}(T, p) = G_{\text{IrO}_2}(T, p) - G_{\text{Ir}}(T, p) - 2\mu_{\text{O}}(T, p) \quad (5)$$

We have optimized the structures of a bulk IrO<sub>2</sub> oxide (rutile structure) and of bulk Ir using DFT, and the total energies of the two systems have been obtained. As above, we use the DFT-calculated total energy to represent the corresponding free energy of the solid state,  $G_{\text{IrO}_2}$  and  $G_{\text{Ir}}$ . By incorporating the known  $\mu_{\text{O}}(T, p)$  into eq 5, we obtain  $\delta G_{\text{ox}}(600 \text{ K}, 0.08 \text{ atm}) = -0.95 \text{ eV}$ .

Considering that the system (Ir and O<sub>2</sub>) should be in equilibrium,  $\delta G_{\text{ox}}$  from eq 5 must equal  $2\delta G_{\text{ads}}$  from eq 4. Using  $2\delta G_{\text{ads}} = \delta G_{\text{ox}} = -0.95 \text{ eV}$ , we can obtain that the  $E_{\text{ad}}^{\text{diff}}$  is 3.95 eV. Since the 3.95 eV value is larger than the 3.47 eV obtained above, it is indicated that the oxide may start to form before the thermodynamic O saturation coverage on the surface is reached. When the O adsorption energy on Ir is larger than 3.95 eV, O<sub>2</sub> dissociatively adsorbs on the surface; when the O adsorption energy is below 3.95 eV, O adatoms will dissolve into the bulk to form oxide. One obvious way to prevent this is to add reductants. The presence of reductants can deplete the surface O atoms so as to reduce the possibility of oxide formation (as discussed in section 3.4). It may also be borne in

(29) Ge, Q. F.; Kose, R.; King, D. A. *Adv. Catal.* **2000**, *45*, 207.

(30) Michaelides, A.; Liu, Z.-P.; Zhang, C. J.; Alavi, A.; King, D. A.; Hu, P. J. *Am. Chem. Soc.* **2003**, *125*, 3704.

(31) Michaelides, A.; Bocquet, M.-L.; Sautet, P.; Alavi, A.; King, D. A. *Chem. Phys. Lett.* **2002**, *367*, 344.

(32) Reuter, K.; Scheffler, M. *Phys. Rev. B* **2001**, *65*, 035406.

(33) *CRC Handbook of Chemistry and Physics*, 79th ed.; CRC Press: Boca Raton, FL, 1998–1999.



**Table 1.** Adsorption Energies (Unit: eV) of N, O, and NO on Ir{211} and Ir{111} Surfaces

site	Ir{211}							Ir{111}		
	SF	SH	SB	4H	TF	TH	TT	hcp	fcc	top
NO	1.91	2.40	3.14	unstable	1.78	1.92	1.81	2.10	2.09	1.85
N	4.61	5.31	5.51	4.87	4.57	4.66	unstable	5.16	5.01	3.17
O	4.46	4.86	5.39	unstable	4.11	4.10	unstable	4.51	4.73	3.24

mind that the real catalytic system may well not exist in thermodynamic equilibrium, due to the presence of other gas components. For instance, it is expected that the oxide formation process (e.g. surface O dissolving into bulk) is kinetically slow compared to the O-removal reactions or the  $\text{NO} + \text{O} \rightarrow \text{NO}_2$  reaction that occurs on the surface. This is particularly true at lower temperatures: experiments have shown that metal catalysts can stay in the reduced form when hydrocarbons are used as reductants.<sup>4,13,16</sup>

**3.2. NO, N, and O Adsorption on Clean Ir and O-Covered Ir Surfaces.** According to the thermodynamic considerations outlined above,  $E_{\text{ad}}^{\text{diff}}$  is an indexical quantity linked to the phase of the  $\text{O}_2 + \text{Ir}$  system. In the following, DFT calculations will be employed to quantitatively determine  $E_{\text{ad}}(\text{O})$ , as well as the O effects on the adsorption of other adsorbates. As a starting point, we first studied the adsorption of NO, O, and N on the clean Ir{111} and Ir{211} surfaces, which serve as a reference system for later comparisons. The coverage of the adsorbate calculated is 0.25 ML on Ir{111} (one adsorbate per  $p(2 \times 2)$  unit cell, Figure 1a) and 0.50 ML on Ir{211} (one adsorbate per  $(1 \times 2)$  unit cell, Figure 1b). At these coverages the adsorbates do not share bonding with their periodic images. It might be noticed that the 0.50 ML coverage on Ir{211} is a quite low coverage. This is because Ir{211} is a stepped surface with the second and third layer metal atoms being exposed, which leads to the saturation coverage of adsorbate being usually much higher than 1 ML. The calculated adsorption energies ( $E_{\text{ad}}$ )<sup>34</sup> of NO, N, and O adsorption on a series of high-symmetry sites on Ir{111} and Ir{211} (labeled in Figure 1) have been listed in Table 1. We found that on the flat {111} surface the three-fold hollow sites are the most stable for all three species: N adatoms prefer the hexagonal close-packed (hcp) hollow site; O adatoms prefer the fcc hollow site; and NO molecules have a similar adsorption energy on the two hollow sites. On the stepped {211} surface the two-fold step-bridge (SB) site is the most stable site for all the species. We also found that the stepped {211} surface can bond the adsorbate more strongly than the flat {111} surface, which is consistent with the general consensus of the enhanced bonding ability of steps. This enhanced bonding ability results from the low coordination of step-edge metal atoms.<sup>20,23</sup>

Next, we increased the oxygen coverage,  $\theta_{\text{O}}$ , on both Ir{111} and Ir{211} in order to examine the variation of  $E_{\text{ad}}(\text{O})$  with respect to  $\theta_{\text{O}}$ . The coverages investigated are shown in Table 2. We have determined the most stable O adsorption configuration for each  $\theta_{\text{O}}$ , and the corresponding  $E_{\text{ad}}(\text{O})$  was calculated. The  $E_{\text{ad}}(\text{O})$  at a given coverage,  $\theta_{\text{O}}^{\alpha}$ , is calculated to be the energy gain when adding a  $\theta_{\text{O}}^{\text{unit}}$  ML O atoms (isolated in a

**Table 2.** Adsorption of O Atoms on Ir{211} and Ir{111} Surfaces at Different Coverages<sup>a</sup>

	Ir{211}				Ir{111}	
	0.50	1.00	1.50		0.25	0.50
$\theta_{\text{O}}$ (ML)	SB	SB + SF	SB + SB + TH		fcc	fcc + fcc
$E_{\text{ad}}(\text{O})$ (eV)	5.39	4.29	4.10		4.73	4.23
$\Delta E_{\text{ad}}$ (eV)	0	−1.10	−1.29		−0.66	−1.16

<sup>a</sup>  $\Delta E_{\text{ad}}$  is the difference of  $E_{\text{ad}}(\text{O})$  with respect to the highest  $E_{\text{ad}}(\text{O})$ , i.e.,  $E_{\text{ad}}(\text{O})$  of the 0.50 ML O on Ir{211}.

vacuum) onto the  $(\theta_{\text{O}}^{\alpha} - \theta_{\text{unit}})$  ML O-covered surface (here  $\theta_{\text{unit}} = 0.50$  ML for the Ir{211} and  $\theta_{\text{unit}} = 0.25$  ML for the Ir{111}). By this definition,  $E_{\text{ad}}(\text{O}) \approx E_{\text{ad}}^{\text{diff}}$ , the differentiation adsorption energy in eq 4.<sup>35</sup> Table 2 shows that  $E_{\text{ad}}(\text{O})$  decreases continuously on both surfaces as the  $\theta_{\text{O}}$  increases, which reflects a repulsive interaction between the O atoms. It should be mentioned that, from Table 1, at all the O coverages studied, up to 1.5 ML on Ir{211} and 0.50 ML on Ir{111},  $E_{\text{ad}}(\text{O})$  is larger than 3.95 eV. This implies that  $\text{IrO}_2$  will not form until a higher O coverage is built up. Because the stepped Ir{211} surface is of more interest for its high reactivity according to our previous study,<sup>22</sup> we highlighted the structures of the 0.50, 1.0, and 1.50 ML O-covered Ir{211} in Figure 2 a, b, and c, respectively. Figure 2a–c shows that the O atoms occupy the stepped sites initially, and with the increase of  $\theta_{\text{O}}$  they start to appear on terraces.

By adding NO and N onto the O-covered Ir surfaces, we were able to investigate the O effects on the coadsorbed NO and N. On the basis of the potential energy surface on the clean surface (Table 1), we have explored the most likely coadsorption configurations (the O adsorption site is also allowed to vary), and the most stable structures for these coadsorption systems were then mapped out. For example, for the NO adsorption on the 0.50 ML O-covered Ir{211}, we studied six different combinations, namely SB(NO) + SB(O), SH(NO) + SB(O), TH(NO) + SB(O), SB(NO) + SH(O), SB(NO) + SF(O), and SH(NO) + SH(O), and the configuration of SB(NO) + SB(O) is found to be the most stable. Figure 2d,e highlights the adsorption structures of the NO and N on the 0.50 ML O-covered Ir{211}. The calculated  $E_{\text{ad}}$  values of NO and N on the surfaces have been listed in Table 3. Table 3 shows that the presence of O adatoms weakens the bonding of the NO and N, indicating a repulsive interaction between the O atom and the incoming NO or N. Interestingly, the reduction of  $E_{\text{ad}}$  ( $\Delta E_{\text{ad}}$ ) due to the presence of O atoms is not a linear function of the O coverage. On Ir{211} there is a critical O coverage, i.e., 0.50 ML, when the adsorbates are destabilized most significantly. For instance, when  $\theta_{\text{O}}$  increases from 0 to 0.50 ML,  $\Delta E_{\text{ad}}(\text{NO})$  is −0.86 eV, and if the  $\theta_{\text{O}}$  further increases to 1.00 ML,  $\Delta E_{\text{ad}}$  (−1.09 eV) remains quite similar.

The adsorption of NO, O, and N on the 0.50 ML O-covered surface constitutes a nice database for a systematic comparison of the O effects on different adsorbates. We have shown that on the clean surface, the NO, O, and N all prefer the SB site; however, on the 0.50 ML O-covered surface they sit at three different sites, namely, NO at the SB site, O at the SF site, and N at the TH site (see Figure 2). This may be rationalized as follows. When Ir{211} is covered by 0.50 ML O, each step-

(34) It should be noticed that  $E_{\text{ad}}$  from the DFT-slab calculation is an integral adsorption energy over a coverage range,<sup>29</sup> which is not exactly the same as the differential adsorption energy  $E_{\text{ad}}^{\text{diff}}$  (see eq 4). As far as the  $E_{\text{ad}}^{\text{diff}}$  is a decreasing function of coverage  $\theta$ , the integral adsorption energy  $E_{\text{ad}}$  at a coverage is always larger than the  $E_{\text{ad}}^{\text{diff}}$  at the same coverage (see ref 29).

(35) By the definition, as  $\theta_{\text{unit}}$  becomes infinitely small,  $E_{\text{ad}}$  will approach the differential adsorption energy  $E_{\text{ad}}^{\text{diff}}$ .

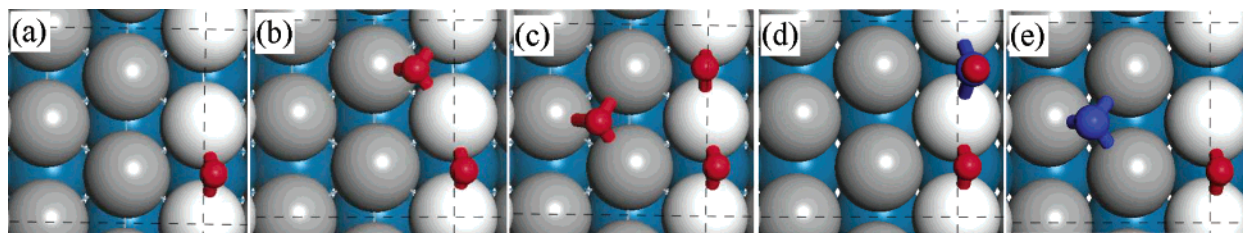


**Figure 2.** Calculated structures of the O-covered Ir{211} at 0.50 (a), 1.00 (b), and 0.50 (c) ML O coverages, as well as the NO (d) and N (e) adsorption on the 0.50 ML O-covered Ir{211}. The O and N atoms are represented by red and blue balls, respectively.

**Table 3.** Adsorption of NO and N on the O-Covered Ir{211} and Ir{111}<sup>a</sup>

	$\theta_{\text{O}}$ (ML)	Ir{211}			Ir{111}	
		0	0.50	1.00	0	0.25
NO	site	SB	SB (O: SB)	SB (O: SB+TH)	hcp	top (O: fcc)
	$E_{\text{ad}}$	3.14	2.28	2.05	2.10	1.95
	$\Delta E_{\text{ad}}$	0	-0.86	-1.09	-1.04	-1.19
N	site	SB	TH (O: SB)	TH (O: SB+SB)	hcp	fcc (O: fcc)
	$E_{\text{ad}}$	5.51	4.60	4.57	5.16	4.39
	$\Delta E_{\text{ad}}$	0	-0.91	-0.94	-0.35	-1.12

<sup>a</sup> The adsorption sites of the coadsorbed O are indicated in parentheses. The  $\Delta E_{\text{ad}}$  of NO/N is the difference of a  $E_{\text{ad}}(\text{NO}/\text{N})$  with respect to the highest  $E_{\text{ad}}(\text{NO}/\text{N})$ , i.e.,  $E_{\text{ad}}(\text{NO}/\text{N})$  on the clean Ir{211}.

edge Ir atom is bonded to one O atom (Figure 2a). Consequently, the adsorption of any incoming adsorbate on the surface will face two most likely situations: (i) sitting near the steps but *sharing bonding* with the coadsorbed O, in which situation the adsorption is at the expense of an energy cost due to the so-called *bonding competition effect* (denoted as  $E_{\text{bc}}$ ); or (ii) sitting at the terrace sites to avoid the coadsorbed O, in which case the adsorption on terraces is less stable compared to that on the clean stepped sites (the energy cost is denoted as  $\Delta E_{\text{Step-Ter}}$ ). Therefore, in both cases the  $E_{\text{ad}}$  of the adsorbate is reduced on the O-covered surface. The adsorption site of the adsorbate on the O-covered surface is thus determined by the difference between the  $E_{\text{bc}}$  and the  $\Delta E_{\text{Step-Ter}}$  ( $E_{\text{bc}} - \Delta E_{\text{Step-Ter}}$ ). The computation of these two quantities is described in the following.

To calculate the  $E_{\text{bc}}$  of the adsorbate (NO, N, or O), we forced the incoming adsorbate to sit at the SB site on the 0.50 ML O-covered surface (the adsorbed O atom sits at another SB site). In this structure, the adsorbate shares bonding with the nearby O atom. The  $E_{\text{bc}}$  is the energy difference between the  $E_{\text{ad}}$  of the adsorbate on the O-covered surface and the  $E_{\text{ad}}$  of the same adsorbate on the clean surface. We found that the  $E_{\text{bc}}$  is 0.86, 1.13, and 1.58 eV for the NO, O, and N species, respectively. Obviously, the bonding competition of the N - - O pair is the largest and that of the NO - - O pair is the smallest. The  $\Delta E_{\text{Step-Ter}}$  can be obtained directly from Table 1, which gives 1.22, 1.28, and 0.85 for the NO, O, and N species, respectively. In total, the value of the ( $E_{\text{bc}} - \Delta E_{\text{Step-Ter}}$ ) increases monotonically from the NO (-0.36 eV), to the O (-0.15 eV), and to the N (0.73 eV) adsorption. Therefore, it can readily be deduced that, on going from the NO, to the O, and finally to the N adsorption, the adsorbate should be gradually repelled from the SB site to the terrace sites, because of the rapid increasing of  $E_{\text{bc}}$ , the bonding competition energy cost.

**3.3. O-Poisoning Effects on NO Reduction.** NO adsorption has been conducted in experiments on several Ir single-crystal surfaces.<sup>3,36–38</sup> The general consensus is as follows: (i) at low temperatures NO adsorbs molecularly; (ii) at elevated temper-

atures, NO starts to dissociate into N and O atoms on the surface; and (iii) at high NO exposures, the dissociated N and O adatoms reach saturation on the surface and NO then adsorbs only molecularly. On Ir{111},<sup>36</sup> the starting temperature for dissociation is about 350 K. On the ridged Ir{110}<sup>37</sup> and the open Ir{100}-(1×1)<sup>38</sup> surfaces, NO dissociation is easier, starting below 300 K. These surface science studies showed clearly that NO dissociation is inhibited at high O coverages. For NO reduction, however, the ability of a catalyst to dissociate NO is not enough; the selectivity is also highly important. It remains unclear whether, and if so how, the activity and the selectivity of NO reduction are modified by low O coverages. In the following we will use 0.50 ML O-covered Ir{211} as a model system to study the effect of O on NO reduction.

We have calculated the  $\text{NO} \leftrightarrow \text{N} + \text{O}$ ,  $\text{N} + \text{N} \rightarrow \text{N}_2$ ,  $\text{NO} + \text{N} \rightarrow \text{N}_2\text{O}$ , and  $\text{NO} + \text{O} \rightarrow \text{NO}_2$  reactions on 0.50 ML O-covered Ir{211} and have compared with the results on the clean Ir{211} surface. The most stable transition states for these reactions have been located (the coadsorbed O atoms were fully relaxed during the search for the TSs), and the optimized structures are shown in Figure 3. We have found that the TS structure of each reaction on the O-covered Ir{211} is, in general, very similar to that on the clean surface. One major difference lies in the fact that the TS complex on the O-covered surface has always to share bonding with the coadsorbed O atoms (see Figure 3), which is expected to weaken the TS complex bonding with the surface due to the bonding competition effect. In addition, we also noticed that the reaction coordinate (the length of the bond being formed/broken) of the TS on the O-covered surface is generally longer compared to that of the TS on the clean surface. For example, the N–O distance of the TS for  $\text{NO} \rightleftharpoons \text{N} + \text{O}$  reaction on the O-covered surface is 1.74 Å, while it is 1.60 Å for the TS on the clean surface. It is indicated that the presence of the coadsorbed O adatoms modifies the “timing” of the TS being achieved, pushing it “later” in the path from bonded to nonbonded.

With respect to the most stable initial state (IS) and the final state (FS) (Tables 2 and 3), the activation energy  $E_a$  for each reaction was then determined; these values are listed in Table 4 together with those on clean Ir{211}.<sup>22</sup> It can be seen that the  $E_a$  for NO dissociation is almost constant with or without the coadsorbed O, and that the  $E_a$  for all the association reactions are much reduced on the O-covered surface. A closer look, however, reveals that the magnitude of the  $E_a$  reduction ( $\Delta E_a$  in Table 4) for the association reactions is not quite uniform.

- (36) Davis, J. E.; Karseboom, S. G.; Nolan, P. D.; Mullins, C. B. *J. Chem. Phys.* **1996**, *105*, 8326.  
 (37) deWolf, C. A.; Bakker, J. W.; Wouda, P. T.; Nieuwenhys, B. E.; Baraldi, A.; Lizzit, S.; Kiskinova, M. *J. Chem. Phys.* **2000**, *113*, 10717.  
 (38) Gardner, P.; Martin, R.; Nalezinski, R.; Lamont, C. L. A.; Weaver, M. J.; Bradshaw, A. M. *J. Chem. Soc., Faraday Trans.* **1995**, *91*, 3575.

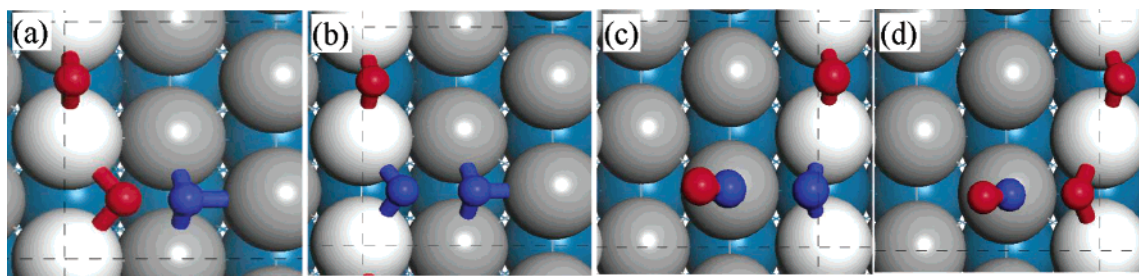


**Figure 3.** Optimized TS structures for the  $\text{NO} \leftrightarrow \text{N} + \text{O}$ ,  $\text{N} + \text{N} \rightarrow \text{N}_2$ ,  $\text{NO} + \text{N} \rightarrow \text{N}_2\text{O}$ , and  $\text{NO} + \text{O} \rightarrow \text{NO}_2$  reactions on the 0.50 ML O-covered Ir{211}. The O and N atoms are represented by small red and blue balls, respectively.

**Table 4.** Barriers ( $E_a$ , Unit: eV) for the  $\text{NO} \leftrightarrow \text{N} + \text{O}$ ,  $\text{N} + \text{N} \rightarrow \text{N}_2$ ,  $\text{NO} + \text{N} \rightarrow \text{N}_2\text{O}$ , and  $\text{NO} + \text{O} \rightarrow \text{NO}_2$  Reactions on the Clean and the 0.50 ML O-covered Ir{211} (O/Ir{211}) Surface<sup>a</sup>

	$E_a(\text{Ir}\{211\})$	$E_a(\text{O/Ir}\{211\})$	$\Delta E_a$
$\text{NO} \rightarrow \text{N} + \text{O}$	1.19	1.16	−0.03
$\text{N} + \text{O} \rightarrow \text{NO}$	2.31	1.13	−1.18
$\text{N} + \text{N} \rightarrow \text{N}_2$	1.81	1.20	−0.61
$\text{N} + \text{NO} \rightarrow \text{N}_2\text{O}$	2.31	1.60	−0.71
$\text{NO} + \text{O} \rightarrow \text{NO}_2$	2.56	1.11	−1.45

<sup>a</sup>  $\Delta E_a$  is the  $E_a$  change on going from the clean to the O-covered surface.

The  $\Delta E_a$  values for the oxidative reactions,  $\text{N} + \text{O} \rightarrow \text{NO}$  and  $\text{NO} + \text{O} \rightarrow \text{NO}_2$ , are much more pronounced (more than 1.1 eV) compared to those for the nitrification reactions,  $\text{N} + \text{N} \rightarrow \text{N}_2$  and  $\text{NO} + \text{N} \rightarrow \text{N}_2\text{O}$  ( $\sim 0.6$  eV). It should be pointed out that, on the O-covered surface, the NO dissociation is still not fully hindered but becomes nearly thermoneutral (0.03 eV endothermic); the NO dissociation and NO formation consequently have similar barriers. This is in contrast to the situation on the clean Ir{211} surface, where the  $\text{NO} \rightarrow \text{N} + \text{O}$  reaction is strongly exothermic by 1.12 eV, and thus the dissociation reaction is favored over the reverse association reaction. It is expected that further increasing the O coverage would render the NO dissociation reaction thermodynamically impossible, as suggested by Bradley et al.,<sup>39</sup> and the Ir catalyst will eventually lose catalytic ability. In the thermoneutral case, however, net NO reduction would remain possible, so long as barriers to the formation of  $\text{N}_2\text{O}$  or  $\text{N}_2$  remain lower than those to the formation of NO or  $\text{NO}_2$ .

Having seen the pronounced barrier changes, one would expect that both the activity and the selectivity for the NO reduction on the O-covered surface will be quite different from those on the clean surface. First, the tendency of NO dissociation is much reduced because the barriers to NO dissociation and NO formation are similar. This leads to a much lower concentration of N atoms on the surface. Second, the  $\text{N}_2$  formation ( $E_a = 1.20$  eV) is not much easier compared to the NO formation ( $E_a = 1.16$  eV). Third, the  $\text{NO} + \text{O} \rightarrow \text{NO}_2$  reaction becomes highly competitive with NO dissociation because of their similar barriers. Consequently, the adsorbed NO molecules can be oxidized to  $\text{NO}_2$  well before they have the chance to dissociate. Combining all the changes, it appears that the reduction of NO will be difficult on the O-covered surface, but the oxidation to  $\text{NO}_2$  will be more likely. This is in accord with the experiment finding<sup>13</sup> that, in the absence of reductants,  $\text{NO}_2$  is the major product for NO treatment under excess  $\text{O}_2$  conditions.

**Table 5.** Adsorption of H, CO, C, and CH Species on the Ir{111} and Ir{211} Surfaces<sup>a</sup>

adsorbate	{211}		{111}	
	site	$E_{\text{ad}}$	site	$E_{\text{ad}}$
H	SB	3.27	top	2.86
CO	ST	2.79	top	2.29
C	4H	7.79	hcp	7.43
CH	4H	7.32	hcp	7.11

<sup>a</sup> The most stable site and the corresponding adsorption energy ( $E_{\text{ad}}$ , unit: eV) are listed.

Here we should mention an important experimental study by Bradley, Hopkinson, and King<sup>39</sup> on ammonia oxidation<sup>40</sup> on Pt{100}, where two competitive surface processes, NO and  $\text{N}_2$  formation, are involved. Using the molecular-beam technique, they found that above a critical O coverage,  $\sim 0.2$  ML, the reaction pattern is switched from  $\text{N}_2$  formation to NO formation.<sup>39</sup> This experimental result is consistent with our current calculations. On clean Ir{211},  $\text{N}_2$  formation is the main reaction channel, but on the 0.50 ML O-covered surface, NO and  $\text{NO}_2$  formation turn out to be more competitive.  $\text{NO}_2$  is the major product in the present case, however, because of the high surface concentration of NO and O.

**3.4. O-Removal Reactions: Preventing Catalysts from O Poisoning.** The above results show that the poisoning of the catalyst by O is inevitable in the absence of reductants. To understand the working mechanisms of reductants, we need to study the O-removal reactions, in which reductants or their surface derivatives take part. For the reductants  $\text{H}_2$  and CO, and for the dissociation products of various different hydrocarbons, the following four O-removal reactions are most likely to be involved:  $\text{H} + \text{O} \rightarrow \text{OH}$ ,  $\text{CO} + \text{O} \rightarrow \text{CO}_2$ ,  $\text{C} + \text{O} \rightarrow \text{CO}$ , and  $\text{CH} + \text{O} \rightarrow \text{HCO}$ . The  $\text{H} + \text{O} \rightarrow \text{OH}$  and  $\text{CO} + \text{O} \rightarrow \text{CO}_2$  reactions are the elementary step for the reductants  $\text{H}_2$  and CO to remove the surface O atoms, respectively. Aside from the  $\text{H} + \text{O}$  reaction, the  $\text{C} + \text{O}$  and  $\text{CH} + \text{O}$  reactions are the most likely O-removal reactions in which hydrocarbons participate. This is because, at realistic reaction temperatures (e.g. 600 K), hydrocarbons (including alkanes and alkenes) will have decomposed into C adatoms (perhaps some CH species) and H atoms on the surface, as observed in experiment.<sup>13,16,23</sup>

Before investigating these O-removal reactions, we first determined the potential energy surfaces of the C, CH, CO, and H species on Ir{111} and Ir{211}. In Table 5 we listed the most stable adsorption site and the corresponding  $E_{\text{ad}}$  of these species on the Ir surfaces. It can be seen that the C and CH species always prefer the high-coordination sites, i.e., four-fold hollow site on steps, three-fold hcp hollow site on Ir{111}. On the other hand, the H and CO prefer the low-coordination sites, e.g. the top site. Similar to the N, O, and NO species (Table 1),

(39) Bradley, M.; Hopkinson, A.; King, D. A. *J. Phys. Chem.* **1995**, 99, 17032.



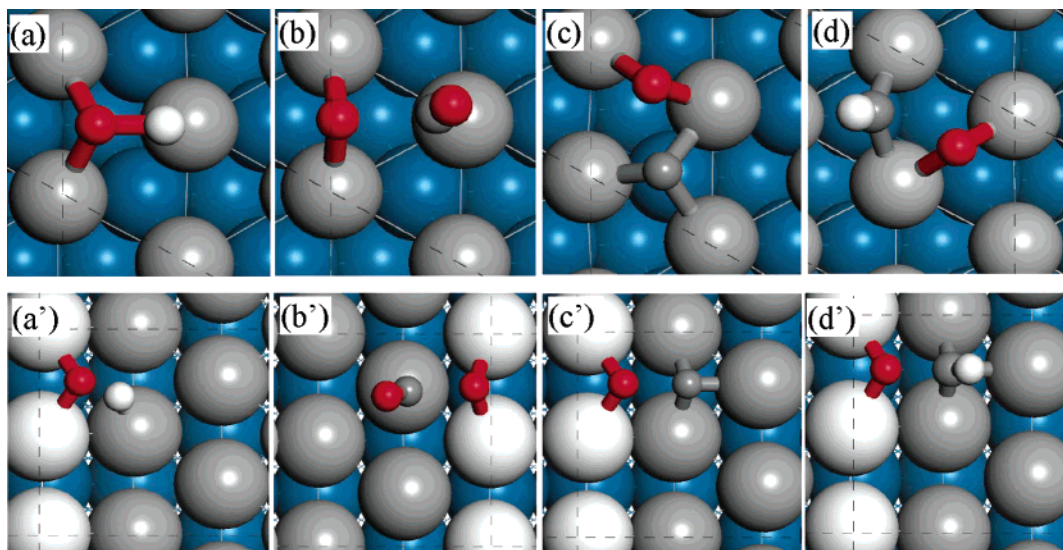


**Figure 4.** Optimized TS structures for the  $\text{H} + \text{O} \rightarrow \text{OH}$  (a, a'),  $\text{CO} + \text{O} \rightarrow \text{CO}_2$  (b, b'),  $\text{C} + \text{O} \rightarrow \text{CO}$  (c, c'), and  $\text{CH} + \text{O} \rightarrow \text{HCO}$  (d, d') reactions on the Ir{111} (upper panel) and Ir{211} (bottom panel) surfaces. The O, C, and H atoms are represented by small red, gray, white balls, respectively.

**Table 6.** Reaction Barriers (Unit: eV) for  $\text{H} + \text{O} \rightarrow \text{OH}$ ,  $\text{CO} + \text{O} \rightarrow \text{CO}_2$ ,  $\text{C} + \text{O} \rightarrow \text{CO}$ , and  $\text{CH} + \text{O} \rightarrow \text{HCO}$  on the Clean Ir{111} and the Stepped Ir{211}<sup>a</sup>

	$E_a^{(111)}$	$E_a^{(211)}$	$\Delta E_a$	$r_{(211)}/r_{(111)}$
$\text{H} + \text{O} \rightarrow \text{OH}$	1.30	1.21	−0.09	5.9
$\text{CO} + \text{O} \rightarrow \text{CO}_2$	1.35	1.70	0.35	$10^{-3}$
$\text{C} + \text{O} \rightarrow \text{CO}$	2.17	1.54	−0.63	$10^6$
$\text{CH} + \text{O} \rightarrow \text{HCO}$	1.84	1.69	−0.15	20

<sup>a</sup>  $\Delta E_a = E_a^{(211)} - E_a^{(111)}$ ;  $r_{(211)}/r_{(111)}$  is the ratio of the reaction rates ( $r$ ) of the reaction on two surfaces at 600 K assuming the same pre-exponential factors.

the C, CH, H, and CO species also adsorb more strongly on the step than they do on the flat surface.

Next, we searched for the reaction pathways of the four oxidation reactions:  $\text{H} + \text{O} \rightarrow \text{OH}$ ,  $\text{CO} + \text{O} \rightarrow \text{CO}_2$ ,  $\text{C} + \text{O} \rightarrow \text{CO}$ , and  $\text{CH} + \text{O} \rightarrow \text{HCO}$  on clean Ir{111} and Ir{211}. The optimized TS structures for them have been shown in Figure 4. The  $E_a$  of each reaction has been calculated with respect to the most stable IS and is shown in Table 6. Table 6 shows two important features of these O-removal reactions. First, all the O-removal reactions can proceed with a barrier lower than the  $E_a$  to  $\text{N}_2$  formation (1.81 eV), either on the flat {111} or on the stepped {211} surface. This indicates that at the reaction temperatures all the O-removal reactions are reactive enough to remove O adatoms. More importantly, the barrier difference on two surfaces ( $\Delta E_a = E_a^{(211)} - E_a^{(111)}$ ) is a value strongly dependent on reactions. For instance, the barrier of the  $\text{C} + \text{O}$  reaction on the step is much smaller than its barrier on the flat surface ( $\Delta E_a = -0.63$  eV). Opposite to the  $\text{C} + \text{O}$  reaction, the  $\text{CO} + \text{O}$  reaction has a barrier on the step higher than that on the flat {111} surface ( $\Delta E_a = 0.35$  eV).

Since the pre-exponential factors of surface reactions are known to be quite constant from surface to surface<sup>41</sup> (usually  $\sim 10^{13}$ ), the ratio of the reaction rate ( $r$ ) of each reaction on the two surfaces ( $r_{(211)}/r_{(111)}$ ) at a reaction temperature, e.g. 600 K, can be calculated on the basis of the Arrhenius law. As shown in Table 6, the  $r_{(211)}/r_{(111)}$  for the O-removal reactions follows

the order of  $\text{C} + \text{O} > \text{CH} + \text{O} > \text{H} + \text{O} > \text{CO} + \text{O}$ . Obviously, this order reflects to what extent the reactions prefer to occur on steps. It should be emphasized that the selectivity of a reductant to react with O adatoms at steps is crucial. First, the step is the active site for NO reduction. Second, the reductant has a much smaller concentration compared to that of the  $\text{O}_2$ . For these two reasons, the reductant needs to be, ideally, consumed maximally at the step but minimally at the flat surface, so as to sustain the catalytic ability of the catalyst.

On the basis of our results, we can rationalize the observed reductant sensitivity of NO reduction as follows. Reductants such as CO and  $\text{H}_2$  are ineffective because they are very active to react with the O atoms on the flat {111} surface and will be largely consumed before they can react with the O atoms on steps. The NO reduction is therefore poisoned with the O accumulation on steps. Between CO and  $\text{H}_2$ , CO is even worse than  $\text{H}_2$  in its selectivity to react with the O atoms on steps, which is consistent with experiment.<sup>13</sup> In contrast, C adatoms can selectively react with the O atoms on steps. The barrier of the  $\text{C} + \text{O}$  reaction on the flat surface is much too high to proceed (2.17 eV), indicating that C adatoms will hardly be consumed by O on the flat {111} surface; the  $\text{C} + \text{O}$  reaction will occur almost exclusively at steps. In other words, even a small amount of C adatoms may sustain the catalytic activity of Ir catalysts. Thus, *the catalytic performance of a reductant is linked with its efficiency to decompose into C atoms*. As unsaturated hydrocarbons, such as alkenes, have a high sticking probability and decompose readily on metals, it is little wonder that they are much more efficient reductants than alkanes. It may also be stressed that H atoms from hydrocarbons can additionally help to prevent the flat surface from being deep-oxidized. In fact, H atom is the species that can most efficiently remove O atoms on the flat {111} surface, as the  $\text{H} + \text{O}$  reaction possesses the lowest barrier among all the O-removal reactions on Ir{111}.

#### 4. Analyses and Discussions

**4.1. Physical Origin of O Poisoning.** In section 3.3, we identified that the adsorbed O atoms affect the barriers of reactions quite differently. Fundamentally, the barrier change

(40) Kim, M.; Pratt, S. J.; King, D. A. *J. Am. Chem. Soc.* **2000**, 122, 2409.

(41) Eichler, A. *Surf. Sci.* **2002**, 498, 314.



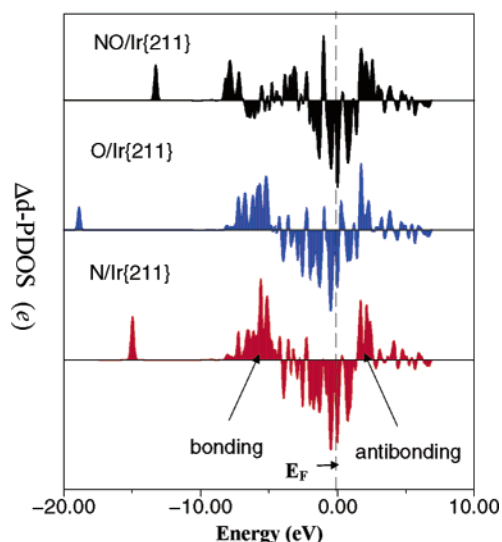


**Figure 5.** Plots of the difference of the d-states' projected density of states ( $\Delta d$ -PDOS) of a step-edge Ir metal (on Ir{211}) before and after the adsorption of NO, O, and N, respectively (also see text). The adsorption site of NO, O, and N is the SB site on Ir{211}. All the  $\Delta d$ -PDOSs are lined up with the Fermi level ( $E_F$ ), which is set to be energy zero.

for a reaction is originated from the different extent of the destabilization of the reactants, products, and TS complexes by the coadsorbed O. Therefore, in this part we will address first why the destabilization due to the coadsorbed O adatoms is adsorbate-dependent. On this basis, the barrier changes of the reactions in the NO reduction will be analyzed.

**4.1.1. O Poisoning on the Adsorption of Different Adsorbates.** We start from a comparison of the bonding of three different adsorbates, NO, O, and N, on Ir{211}. For the adsorbate of small molecules and electronegative atoms (e.g. NO, CO, and O) on transition metals, previous studies have suggested that a large portion of the adsorbate–metal bonding is achieved through the orbital mixing between the adsorbate valence states and the metal d-states.<sup>41–45</sup> Accordingly, we have performed the following analysis on the change of metal d-states before and after adsorption. First, we have calculated the d-states' projected density of states ( $d$ -PDOS) of a step-edge Ir atom on clean Ir{211}. The  $d$ -PDOS has been normalized to the total 10-electron limit of the d-states of one Ir atom. Second, we calculated the  $d$ -PDOSs of the same step-edge Ir atom after the adsorption of NO, O, or N on the SB site. By subtracting the  $d$ -PDOS of the clean surface from the  $d$ -PDOS of the adsorption system, we obtained the  $\Delta d$ -PDOSs of NO, O, and N adsorption on Ir{211}, which are plotted in Figure 5.

An obvious common feature in Figure 5 is that the  $\Delta d$ -PDOS around the Fermi level ( $E_F$ ) (in a window of several eV) is strongly negative for all three cases. This is an indication that these d-states of the clean metal are involved mostly in the chemical bonding with the adsorbates and are thus shifted in energy upon adsorption. For the N and O atoms bonding on Ir{211}, two broad regions with positive  $\Delta d$ -PDOS can be

**Table 7.** d Population Difference ( $\Delta n_d$ ) and Energy Change of the d Electrons ( $E_d$ ) of a Step-Edge Ir Atom (Ir{211}) before and after the Adsorption of NO, O, and N, Respectively<sup>a</sup>

	NO/Ir{211}	O/Ir{211}	N/Ir{211}
$\Delta n_d$ (e)	0.041	−0.124	−0.042
$E_d$ (eV)	−3.76	−4.76	−6.34

<sup>a</sup> The values are calculated using eqs 6 and 7.

distinguished: one comprises occupied states around  $-7$  to  $-5$  eV, and another comprises unoccupied states around  $+2$  eV. These two regions are the main bonding and antibonding regions between the adatom p-states and the metal d-states, respectively, as labeled in the  $\Delta d$ -PDOS of N/Ir{211}. For NO bonding on Ir{211}, the spectrum of the  $\Delta d$ -PDOS is more complex because there are multiple molecular orbitals in NO, i.e.,  $5\sigma$ ,  $1\pi$ ,  $2\pi$ , that mix with metal d-states. Nevertheless, its major antibonding region still appears at a quite similar place ( $+2$  to  $+3$  eV) as those of the N and O adsorptions.

Using Figure 5, we can calculate two important quantities: first, the d population difference before and after adsorption, namely  $\Delta n_d$  from eq 6; second, the energy change of d electrons upon adsorption, namely  $E_d$  from eq 7.

$$\Delta n_d = \int_{-\infty}^{E_F} \Delta n(\epsilon) d\epsilon \quad (6)$$

$$E_d = \int_{-\infty}^{E_F} \Delta n(\epsilon) \epsilon d\epsilon \quad (7)$$

Here,  $\Delta n(\epsilon)$  (the y axis of the  $\Delta d$ -PDOS) is the change of the d-state's electron density at the energy  $\epsilon$ . The  $\Delta n_d$  and  $E_d$  values for the NO, O, and N adsorptions have been calculated and are shown in Table 7. Consistent with chemical common sense, we found that the metal d-states slightly lose electrons upon the adsorption of electronegative N and O atoms; the d-states donate more electrons to the O than to the N because the O is more electronegative. In contrast, the metal d-states gain electrons upon the adsorption of NO. This is also reasonable, considering that NO has one unpaired  $2\pi$  electron, which can be readily donated to the metal surface. Table 7 shows the energy change of d-electrons,  $E_d$ :  $-6.34$  eV in the case of N adsorption,  $-4.76$  eV in the case of O adsorption, and  $-3.76$  eV in the case of NO adsorption. This implies that the extent of the stabilization of d-states after adsorption is in the order  $N > O > NO$ . This is reasonable, considering that the free N atom's valency is 3 (three nonpaired electrons), the O atom's valency is 2 (two nonpaired electrons), and the NO, being a nearly closed-shell molecule, has only one nonpaired electron. It is expected that the high-valency adsorbate can form stronger covalent bonding with the surface, and therefore stabilize the metal d-states to a greater extent.

The above analyses of electronic structure can provide deeper insight into the bonding competition effect.<sup>42</sup> Due to the fact that all the adsorbates bond with the metal d-states around  $E_F$ , a large repulsion mediated by the surface d-states will be induced when two adsorbates bond with the same metal atoms. The extent of the repulsive interaction depends on how strongly the adsorbates tend to bond with the d-states around  $E_F$ , which can be quantitatively measured by  $E_d$ . As shown in section 3.2, the bonding competition repulsion ( $E_{bc}$ ) follows the order  $N - -O > O - -O > O - -NO$ . This is correctly predicted by the order of the  $E_d$  values (Table 7). We also notice that the bonding

- (42) (a) Bleakley, K.; Hu, P. *J. Am. Chem. Soc.* **1999**, *121*, 7644. (b) Mortensen, J. J.; Hammer, B.; Norskov, J. K. *Surf. Sci.* **1998**, *414*, 315.  
 (43) (a) News, D. M. *Phys. Rev.* **1969**, *178*, 1123. (b) Hoffmann, R. *Rev. Mod. Phys.* **1988**, *60*, 601. (c) Shustorovich, E.; Baetzold, R. C.; Muettterties, E. L. *J. Phys. Chem.* **1983**, *87*, 1100.  
 (44) Hu, P.; King, D. A.; Lee, M.-H.; Payne, M. C. *Chem. Phys. Lett.* **1995**, *246*, 73.  
 (45) Hammer, B.; Norskov, J. K. *Surf. Sci.* **1995**, *343*, 211. Hammer, B.; Norskov, J. K. *Adv. Catal.* **2000**, *45*, 6671.

**Table 8.** Destabilization (Unit: eV) of the IS ( $\Delta E_{IS}$ ) and the TS ( $\Delta E_{TS}$ ) of the Reactions in Table 4 Due to the Presence of a 0.50 ML O (Also See Eq 8)

	$\Delta E_{IS}$	$\Delta E_{TS}$	$\Delta E_a$
$\text{NO} \rightarrow \text{N} + \text{O}$	0.86	0.83	−0.03
$\text{N} + \text{O} \rightarrow \text{NO}$	2.01	0.83	−1.18
$\text{N} + \text{N} \rightarrow \text{N}_2$	1.82	1.21	−0.61
$\text{N} + \text{NO} \rightarrow \text{N}_2\text{O}$	1.77	1.06	−0.71
$\text{O} + \text{NO} \rightarrow \text{NO}_2$	1.96	0.51	−1.45

competition interaction has no apparent relationship with the electronegativity of adsorbates, as it is apparently inconsistent with the order of the  $\Delta n_d$  (Table 8). This also confirms that the dipole–dipole interaction is not an important factor for the bonding competition interaction.<sup>42b</sup>

It should be mentioned that the adsorbate–metal bonding is a fundamental topic that has been hotly studied in the past two decades, and many models have been proposed.<sup>43–45</sup> On the basis of the Newns–Anderson model,<sup>43a</sup> Hammer and Norskov<sup>45</sup> suggested that the metal d-band center ( $\epsilon_{d\text{-center}}$ ) can be a good measure of the bonding ability of metals, and it has been successfully applied to explain many experimental findings.<sup>44</sup> The d-band center model states that the lower the  $\epsilon_{d\text{-center}}$ , the more stable the d-band is, and thus the less bonding ability the metal has. In this work, we also examined the  $\epsilon_{d\text{-center}}$  for the clean Ir{211}, NO/Ir{211}, O/Ir{211}, and N/Ir{211} systems, which are −1.80, −2.19, −2.21, and −2.41 eV with respect to  $E_F$ , respectively. Indeed, the d-band centers are shifted down after the adsorption, and qualitatively it is also true that they follow the same order,  $\text{N} < \text{O} < \text{NO}$ , as for  $E_d$  (Table 7). However, it is noticed that the difference between the  $\epsilon_{d\text{-center}}$  of O and NO adsorption is very small, not consistent with the large differences of the adsorptions shown in Figure 5. In fact, this may be understood as follows. After adsorption, the shape of the metal *d*-DOS has been modified to follow the shape of the adsorbate valence DOS. Thus, different adsorbates will give rise to *d*-DOS of different shape. However, the  $\epsilon_{d\text{-center}}$  parameter, being an averaged value, cannot reflect the change in the shape of the d-band (i.e., two different shapes of d-bands can share the same d-band center). Thus, for different adsorbates,  $\epsilon_{d\text{-center}}$  can be quite close, even though their  $E_d$  values are very different. We contend that  $E_d$  represents a better measure of surface bonding ability than does the d-band center.

**4.1.2. O Poisoning on the Reactions at a Low O Coverage.** Now we are in the position to address the key issue: how the O adatoms modify the reactivity of reactions. Let us consider a general surface equilibrium,  $\text{AB} \leftrightarrow \text{A} + \text{B}$ , with a TS  $[\text{A}-\text{B}]^\ddagger$ . The energy profile of the reaction is schematically shown in Figure 6. When the surface is precovered by O atoms, the reactants, products, and TS of the  $\text{AB} \leftrightarrow \text{A} + \text{B}$  reaction are all destabilized, forming a new reaction profile, also shown in Figure 6. Following Figure 6, the change of the barrier ( $\Delta E_a$ ) due to the presence of O can be decomposed into two parts:

$$\Delta E_a = \Delta E_{TS} - \Delta E_{IS} \quad (8)$$

Thus, the changes in the dissociation barrier ( $\Delta E_{a(\text{dis})}$ ) and the association barrier ( $\Delta E_{a(\text{ass})}$ ) should be written as

$$\Delta E_{a(\text{dis})} = \Delta E_{[\text{A}-\text{B}]^\ddagger} - \Delta E_{\text{AB}} \quad (9)$$

$$\Delta E_{a(\text{ass})} = \Delta E_{[\text{A}-\text{B}]^\ddagger} - (\Delta E_{\text{A}} + \Delta E_{\text{B}}) \quad (10)$$

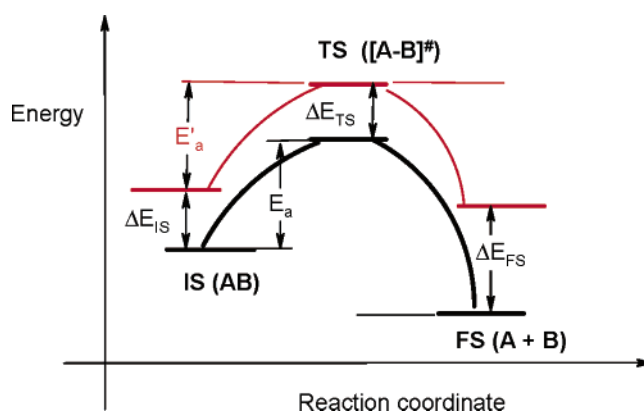


**Figure 6.** Schematic diagram showing the energy profiles of an  $\text{AB} \rightarrow \text{A} + \text{B}$  reaction on the clean surface (black solid curves) and on the O-covered surface (red solid curves).

where  $\Delta E_X$  ( $X = \text{AB}$ ,  $\text{A}$ ,  $\text{B}$ , or  $[\text{A}-\text{B}]^\ddagger$ ) is the adsorption energy change of species  $X$  due to the presence of O.  $\Delta E_{\text{A}}$ ,  $\Delta E_{\text{B}}$ , and  $\Delta E_{\text{AB}}$  can be calculated exactly using DFT;  $\Delta E_{[\text{A}-\text{B}]^\ddagger}$  can then be worked out from eq 9 or 10 once the  $\Delta E_a$  is known. On this basis, we have calculated the individual terms in eq 9 or 10 for the NO dissociation, and for the NO,  $\text{N}_2$ ,  $\text{N}_2\text{O}$ , and  $\text{NO}_2$  formation reactions on the 0.50 ML O-covered Ir{211} surface (Table 5). The results are summarized in Table 8.

Table 8 shows that (i) for the NO dissociation reaction, the O destabilizes the IS and the TS to a similar extent and thus  $\Delta E_{a(\text{dis})}$  is small; and (ii) for all the association reactions, the O destabilization to the IS ( $\Delta E_{\text{A}} + \Delta E_{\text{B}}$ ) is much more significant than that to the TS ( $\Delta E_{[\text{A}-\text{B}]^\ddagger}$ ). As a result, all the association barriers are reduced ( $\Delta E_{a(\text{ass})} < 0$ ). The reason for such a difference between the dissociation and association reactions lies simply with the different number of reactants: there are two reactants in the association reactions and only one in the dissociation reaction. Since the magnitudes of the O destabilization relative to the reactants NO, O, and N are not very different, the more reactants the IS contains, the larger the extent to which the IS is destabilized. (From our results, the 0.50 ML O adatoms reduce the adsorption energy of NO, N, and O by 0.86, 0.91, and 1.10 eV, respectively (Tables 2 and 3), due to the competition of  $E_{bc}$  and  $\Delta E_{\text{Step-Ter}}$ , as discussed in section 3.2.)

Furthermore, it is seen that the  $\Delta E_{TS}$  values in the oxidative reactions are in general smaller than their counterparts in the nitrification reaction:  $\Delta E_{TS}$  of the  $\text{N} + \text{O}$  reaction is 0.38 eV smaller than that of the  $\text{N} + \text{N}$  reaction, and  $\Delta E_{TS}$  of the  $\text{O} + \text{NO} \rightarrow \text{NO}_2$  reaction is 0.55 eV smaller than that of the  $\text{N} + \text{NO}$  reaction. It is this difference, together with the smaller difference in  $\Delta E_{IS}$ , that gives rise to the larger barrier reduction in the oxidative reactions. The larger TS destabilization in the nitrification reactions is a consequence of their larger bonding competition. In Figure 3, we already show that the nitrification reaction has a TS similar to that of the oxidative reaction, namely, in the TS the reacting N or O atom (of the TS complex) sits at the SB site, sharing bonding with the nearby O atoms. Since the bonding competition of  $\text{N}-\text{O}$  is larger than that of  $\text{O}-\text{O}$ , it can be deduced that in the nitrification reactions the TS complexes are destabilized to a larger extent, and so their barrier reductions are smaller.

**4.2. Selectivity of the O-Removal Reactions To Occur in Steps.** In section 3.4, we showed that different O-removal

reactions have distinct preferences as to reaction sites. In particular, the  $C + O$  reaction prefers to occur on steps while the  $CO + O$  reaction occurs dominantly on the flat surface. It is of importance to ask why the reaction site preferences change so significantly from reaction to reaction.

We have compared the TS structures of the  $C + O$ ,  $CH + O$ ,  $H + O$ , and  $CO + O$  reactions (Figure 4). From the TSs of these reactions, they can be divided into two classes. Class I reactions include the  $C + O$ ,  $CH + O$ , and  $H + O$  reactions; class II contains the  $CO + O$  reactions. In class I reactions, the TS structures of the reaction are different on the two surfaces, as shown in Figure 4: on the flat  $\{111\}$  surfaces, one metal atom is shared by the two reactants in the TS, while this does not happen on the  $\{211\}$  surface. Because of the bonding competition effect in the TS on the flat surface, the reaction generally prefers to occur on steps. In class II, the  $CO + O$  reaction, the TSs on the two different surfaces are quite similar, and the two reactants do not share bonding (see Figure 4). Therefore, for class II reactions there is no structural benefit for them to occur on steps. In fact, because the CO and O are more strongly bonded on steps, the barrier of the  $CO + O$  on the step is even higher than that on the flat surface.<sup>30</sup>

One may further expect that the reaction that incurs a larger bonding competition on the flat surface would prefer to occur on steps more strongly. If true, this may explain why the  $C + O$  reaction behaves so differently from the  $H + O$  reaction. Indeed, according to the valency rule outlined in the last subsection, we can understand that the high-valency reactant (such as C, valency 4 as a free atom) will have a larger bonding competition with the O, compared to that of the small-valency reactant (such as H, valency 1) with the O. A similar valency rule has been observed previously on the structure sensitivity of  $CH_4$  and CO dissociation and their reverse reactions.<sup>25</sup>

## 5. Implications for Selective NO Reduction under Excess $O_2$ Conditions

On the basis of the results and the rationalizations presented above, we have obtained some general implications for selective NO reduction under excess  $O_2$  conditions.

**(i) Anti-oxidation Ability of the Catalyst.** Metal catalysts can be deactivated and even oxidized under reaction conditions by excess  $O_2$ . Our thermodynamic calculations showed that the O binding energy at the O saturation coverage is 3.47 eV at 600 K and 0.08 atm  $O_2$  pressure. From previous DFT literature, we know that all transition metals, e.g. Pt, Ir, Rh, and Pd, can bond O with heat larger than 3.47 eV at low O coverages; i.e.,  $O_2$  will dissociatively adsorb on clean transition metals. Since the O poisoning to the NO reduction is found to start at a low O coverage, it is indicated that all the transition metals will be poisoned if no reductants are added. This explains why the traditional three-way catalysts (Rh, Pd, and Pt) do not work for NO reduction under excess  $O_2$  conditions when no hydrocarbons are present. Moreover,  $O_2$  can deep-oxidize the metal to the metal oxide, which will lead to the loss of metal catalyst. To date, 5d metals, Pt and Ir, have been most frequently used in this field, not least because the 5d metals are more stable in the oxidative environment compared to their counterparts in the 4d and 3d metals. From our studies, the anti-oxidation ability of Ir is still not satisfactory because of its thermodynamic tendency toward the oxide formation. In recent years, metal alloys, such

as Cu–Os,<sup>46</sup> Pt–Au,<sup>47</sup> and noble-metal-based catalysts, e.g. Au/ $Al_2O_3$ , have been reported for selective NO reduction. As the alloying of metals may improve significantly the anti-oxidation ability of the pure metals, it points out a new possible direction to search for novel catalysts for selective NO reduction.

**(ii) Surface Structure of the Catalyst.** Together with our previous work,<sup>22</sup> we have demonstrated that the stepped surfaces are the active sites to reduce NO to  $N_2$  on platinum group metals. The presence of the flat surface will yield the byproducts, like  $NO_2$  and  $N_2O$ . Because of the higher surface energy of surface defects compared to the close-packed surfaces, the preparation of catalysts with a high density of surface defects is difficult. To date, growing nanosized small metal particles on supportive oxides is a hot field in heterogeneous catalysis, apparently because the small metal particles contain a significant amount of surface defects and are much more active. For these metal/oxide bimaterial systems, the prevention of sintering of metal particles is another challenging problem.

**(iii) Choice of Reductants.** Due to the readiness of metal catalysts being poisoned by  $O_2$ , reductants are essential for NO reduction. However, not all reductants can work. There are two basic requirements for reductants: first, high selectivity to remove O atoms from metal steps; second, ability to keep catalysts from being deep-oxidized. Among the reductants  $H_2$ , CO, alkenes, and alkanes, only alkenes can satisfy both requirements. They can effectively produce surface C adatoms that do not react with O atoms on the flat surface but do react with O atoms on steps under reaction conditions, keeping the active site available for NO reduction. They also produce H atoms on the surfaces that can help prevent the Ir catalyst being deep-oxidized (the lowest barrier among all O-removal reactions is that for the  $H + O$  reaction). Compared to alkenes, alkanes have much lower sticking probability on metals and therefore are not good candidates for the source of C and H atoms.

## 6. Conclusions

This work represents the first theoretical attempt to obtain a comprehensive picture of selective NO reduction on Ir under excess  $O_2$  conditions. Thermodynamic calculations were used to tackle the possible  $O_2$  effects on Ir catalysts. DFT calculations were then carried out to investigate the O effects on the adsorption of NO, O, and N, and on the NO conversion processes, including NO dissociation and formation,  $N_2$  formation, and the byproduct  $N_2O$  and  $NO_2$  formations. To clarify the catalytic roles of reductants, we have studied  $H + O \rightarrow OH$ ,  $CO + O \rightarrow CO_2$ ,  $C + O \rightarrow CO$ , and  $CH + O \rightarrow HCO$  reactions on the flat Ir $\{111\}$  and the stepped Ir $\{211\}$  surfaces, which are the O-removal reactions instigated by reductants such as  $H_2$ , CO, and hydrocarbons. The reaction pathways and barriers of all these reactions were calculated. On the basis of the understanding achieved, the implications for selective NO reduction under excess  $O_2$  conditions have been discussed in three important aspects: anti-oxidation ability of metal catalysts; surface structure of metal catalysts; and the choice of the reductants.

From thermodynamic calculations, we found that, under reaction conditions of the NO reduction,  $O_2$  will dissociatively

(46) Ozturk, S.; Senkan, S. *Appl. Catal. B.* **2002**, *38*, 243.

(47) Mihut, C.; Descorme, C.; Duprez, D.; Amiridis M. D. *J. Catal.* **2002**, *212*, 125. Mihut C.; Chandler, B. D. *Catal. Commun.* **2002**, *3*, 91.



adsorb on Ir catalysts. Before the O adatoms can reach thermodynamic saturation coverage, when the O adsorption energy is calculated to be 3.47 eV, it is thermodynamically possible for surface O atoms to dissolve into the bulk, forming IrO<sub>2</sub> oxide. The onset of oxide formation occurs when the dissociative adsorption heat (per additional O atom) on the metal surface falls below 3.95 eV. Thermodynamics indicates that the addition of reductants is highly essential, at least for removing surface O atoms to prevent oxide formation.

From the DFT calculations, we have further obtained the following conclusions regarding chemisorption energies of the adsorbates and reaction barriers.

(i) The potential energy surface of seven different species on the clean Ir{111} and Ir{211} surfaces have been determined, including NO, O, N, C, CH, H, and CO species. We have found that the stepped Ir{211} surface bonds all the adsorbates more strongly than the flat Ir{111} surface. Among them, NO has the largest energy preference to the step, of more than 1 eV: the NO adsorption energy on Ir{211} is 3.14 eV, and that on the Ir{111} surface is 2.10 eV. The CH species has the smallest energy change from Ir{111} to Ir{211}: the adsorption energy is 7.11 eV on Ir{111} and 7.32 eV on Ir{211}. The enhanced bonding ability of the step can be rationalized by the fact that the step-edge Ir atom is less coordinated.

(ii) The presence of O on the surface will weaken the bonding of the other adsorbates, such as NO, O, and N species. We have identified a critical O coverage on the Ir{211} surface, i.e., 0.50 ML, where the adsorption of the coadsorbate is destabilized substantially. On further increasing the O coverage, the destabilization remains quite constant. Although NO, O, and N all prefer the step-bridge site on clean Ir{211}, on the 0.50 ML O-covered Ir{211} surface N is driven to the terrace site and is destabilized by 0.91 eV, NO remains at the step-bridge site but is destabilized by 0.86 eV, and O moves to the step-hcp site and is destabilized by 1.10 eV.

(iii) On the 0.50 ML O-covered Ir{211} surface, the activity and selectivity for the NO reduction are significantly modified. We found that although the NO dissociation barrier remains similar with or without the presence of the O, all the association barriers, i.e., the  $N + O \rightarrow NO$ ,  $N + N \rightarrow N_2$ ,  $N + NO \rightarrow N_2O$ , and  $NO + O \rightarrow NO_2$  barriers are greatly reduced, i.e., by 1.18, 0.61, 0.71, and 1.45 eV, respectively. As a result, on the O-covered Ir{211}, NO is mainly oxidized to NO<sub>2</sub> instead of being reduced to N<sub>2</sub> generally on the clean Ir{211}.

(iv) Four different O-removal reactions,  $H + O \rightarrow OH$ ,  $CO + O \rightarrow CO_2$ ,  $C + O \rightarrow CO$ , and  $CH + O \rightarrow HCO$ , have been studied on the clean Ir{111} and Ir{211} surfaces. On going from flat {111} to stepped {211}, the barriers of these reactions are changed by -0.09, 0.35, -0.63, and -0.15 eV, respectively. The  $C + O$  reaction has the largest preference to occur on Ir{211}, while the  $CO + O$  has the least. Because the clean stepped sites are the active site for NO reduction and also reductants are much lower in concentration than O<sub>2</sub>, the preference of an O-removal reaction to occur on the steps is crucial. The high selectivity of the  $C + O$  reaction is responsible for achieving NO reduction under excess O<sub>2</sub> conditions when alkene hydrocarbons are present.

(v) For the adsorption of small molecules and atoms, like NO, O, and N, the valence states of the adsorbates all strongly

mix with the metal d-states around the Fermi level. This common feature of adsorbates is the physical origin for a bonding competition energy cost when two adsorbates bond with the same metal atoms. The bonding competition energy cost is thus determined by the extent of the d-states being perturbed by the adsorbates. We found that the magnitude of the bonding competition of three adsorbate-pairs follows  $N - -O > O - -O > NO - -O$ , which can be explained using a valency rule.

(vi) On the 0.50 ML O-covered Ir{211} surface, the IS, TS, and FS of NO dissociation, and of NO, N<sub>2</sub>, N<sub>2</sub>O, and NO<sub>2</sub> formations reactions, are all destabilized due to the bonding competition effect. In the NO dissociation reaction the barrier is little changed because the IS and the TS are destabilized to a similar extent. In the association reactions the barriers are greatly reduced because the ISs that contain two reactants are much more destabilized than the TS. The O destabilization of the TSs also plays an important role, dictating that the barriers of the oxidative reactions (NO and NO<sub>2</sub> formations) are reduced more significantly than those of the nitrification reactions (N<sub>2</sub> and N<sub>2</sub>O formations).

(vii) For the O-removal reactions, two classes of reactions can be discerned. The class I reactions ( $C + O$ ,  $CH + O$ , and  $H + O$  reactions) generally have lower barriers on steps due to the bonding competition in the TSs on the flat {111} surface. On the basis of a valency rule, we have rationalized why the  $C + O$  reaction is the one that prefers steps the most. The class II reaction (the  $CO + O$  reaction) has similar TS structures on both the flat surface and the step, and thus it does not have a structural benefit to occur on the step. Instead, because the step bonds CO and O more strongly, the  $CO + O$  reaction on the step has an even higher barrier than that on the flat surface.

To recap, we established a comprehensive mechanism of selective NO reduction on Ir under excess O<sub>2</sub> conditions using DFT and thermodynamic calculations. Following our previous paper<sup>22</sup> showing that Ir metal can be both active and selective for NO reduction, here we showed that excess O<sub>2</sub> can easily poison the Ir catalyst and that the addition of reductants is essential. Furthermore, the microscopic mechanism of O<sub>2</sub> poisoning has been elucidated. By comparing a group of reductants that can potentially reduce oxidized Ir, we found that surface C atoms are the key adsorbate to activate the catalyst. Our results explain, for the first time, the fact that heavy hydrocarbons, such as alkenes, are better reductants than small molecules (e.g. CO and H<sub>2</sub>) in NO reduction under excess O<sub>2</sub> conditions. These trends are rationalized by arguments based upon the electronic structure and its contribution toward the bonding competition effect.

**Acknowledgment.** We acknowledge the Isaac Newton Trust (Cambridge) for a postdoctoral fellowship (Z.-P.L.), The Royal Society for a University Research Fellowship (S.J.J.), EPSRC (UK) for computation equipment, and the Cambridge-Cranfield High Performance Computing facility for computer time. We extend our thanks to Dr. S. Matsumoto and colleagues for stimulating discussions.

JA0481833